Staging and follow-up of high-grade malignant salivary gland tumours: The role of traditional versus functional imaging approaches – A review

Nicole Freling [a,*], Flavio Crippa [b], Roberto Maroldi [c]

[a] Department of Radiology, Academic Medical Center, University of Amsterdam, The Netherlands
[b] Department of Nuclear Medicine, Fondazione IRCCS Istituto Nazionale dei Tumori, Milano, Italy
[c] Department of H&N radiology, Head of the Department of Radiology, University of Brescia, Italy

ARTICLE INFO

SUMMARY

Following up on the Consensus Conference on high-grade malignant salivary gland tumours (HGMSGT) in adult patients in Brescia, Italia, in October 2014, we review the current imaging modalities for diagnosing and staging these rare tumours. The advantages of functional MR imaging techniques such as diffusion weighted imaging (DWI) and dynamic contrast-enhanced MR imaging (DCEMRI) in comparison with traditional MRI will be outlined. The limited role of [18]FDG-PET CT and fMRI will be addressed. Finally, in view of new experimental treatment options, we will discuss the role of imaging during follow-up.

© 2016 Elsevier Ltd. All rights reserved.

Introduction

During the Consensus Conference on Salivary Gland Tumours in Brescia, Italia, October 2014, new diagnostic developments in many different fields of clinical research were presented and discussed.

This paper will review current imaging modalities which may contribute to better diagnosis and staging of malignant salivary gland tumours. As in the past, studies on new imaging techniques are hampered by small numbers, due to the rarity of the disease, and by ongoing new developments in imaging, resulting in a paucity of data.

Epidemiology

Salivary gland tumours are rare, accounting for about 2–6.5% of all head and neck tumours and for about 0.5% of all malignancies.

By far the most common location is the parotid gland, with about 70% of tumours arising at this site, followed by – in decreasing order – the submandibular gland, the minor salivary glands and the sublingual gland. Most tumours are benign pleomorphic adenomas (about 65% of all parotid tumours), followed by adenolymphoma or Warthin's tumour (15–20% of all parotid tumours) [1,2]. Malignant epithelial salivary gland tumours are uncommon: the annual incidence rate worldwide is less than 2–3 per 100.000 [3,4]. They account for about 20–30% of parotid tumours, approximately 40% of submandibular gland tumours, 50% of minor salivary gland tumours and 90% of sublingual gland tumours. If left untreated, in 6.5% of cases (range 1.9–23.3%) benign pleomorphic adenomas may dedifferentiate into a high-grade malignant tumour, carcinoma-ex-pleomorphic adenoma [1,5]. Salivary gland tumours are classified according to the World Health Organization (WHO) histologic classification into 31 different types, of which 24 are malignant [3], making final diagnosis a challenge in many cases. The most common low-grade salivary gland tumours are muco-epidermoid carcinoma, adenocarcinoma not otherwise specified (NOS) and acinic cell carcinoma. Many other histologic types do occur, but they are rare [6]. Adenoid cystic carcinoma (ACC) is a high-grade malignant salivary gland tumour (HGMSGT) and is

* Corresponding author at: Department of Radiology, Academic Medical Center, Meibergdreef 9, 1107 AZ Amsterdam, The Netherlands.
  E-mail addresses: n.j.freling@amc.uva.nl (N. Freling), flavio.crippa@istitutotumori.mi.it (F. Crippa), roberto.maroldi@unibs.it (R. Maroldi).

reported as the second most common or fifth most common malignant tumour by different authors [7,1]. Although ACC are known for their slow biological growth, they tend to have a protracted course and final outcome is poor for all grades, with a less than 50% survival rate at 10 years [6]. High grade malignant, non-ACC tumours of the salivary glands are rare and histologically extremely diverse, consisting of high-grade mucoepidermoid carcinoma, adenocarcinoma NOS, carcinoma ex pleomorphic adenoma, myoepithelial carcinoma, anaplastic small cell carcinoma, carcinosarcoma, large cell undifferentiated carcinoma, small cell undifferentiated carcinoma, salivary duct carcinoma and also squamous cell carcinoma (to be differentiated from metastases of CUP).

Non-epithelial malignant tumours represent a minority of malignant salivary gland tumours. Extranodal primary lymphoma of the salivary glands is rare, accounting for only 5% of all extranodal NHL, 2% of all salivary gland tumours [8,9] and 16% of all malignant salivary gland tumours [7,6]. Eighty percent are located in the parotid gland. Bilateral disease is not uncommon. Mucosa-associated lymphoma type (MALT) is the most prevalent histologic subtype. Patients with acquired or drug-induced immunodeficiency (M. Sjoegren) have an increased relative risk for developing parotid MALT lymphoma and also for development of non-Hodgkin lymphoma [10]. Salivary glands are secondarily involved in 1–8% of patients with systemic high grade B-cell NHL, with 80% involving the parotid gland [11].

Mesenchymal malignant tumours make up 1.5% of all malignant salivary gland tumours [6] and include malignant schwannomas, malignant fibrous histiocytomas, solitary fibrous tumours, and rhabdomyosarcomas, among others.

Metastases make up about 10% of all malignant salivary gland tumours. Most (80–90%) are located in the parotid gland. Eighty-percent result from primary tumours elsewhere in the head and neck, only 20% from infraclavicular locations [6,12].

Perineural spread (PNS) is reported in greater than 50% of cases and is particularly common for ACC [1].

Locoregional lymph node metastases from malignant salivary gland tumours are seen in about 10–15% of patients at presentation but are more common (>30%) in high-grade than in low-grade salivary gland tumours [3,13]. Distant metastases occur in about 10–50% of patients at first presentation and may be seen in low and in high T-stages during follow-up [1,14]. In recurrent disease lymph node and distant metastases are more frequently observed [13].

Clinical presentation, family history, imaging and other diagnostic tests are sometimes required to classify a tumour as benign or malignant and in a few equivocal cases only long time follow-up will decide about the clinical behaviour – indolent or aggressive [6]. Although primary surgery is the treatment of choice for salivary gland tumours, curative chemo-radiation has recently become available as a treatment modality when curative surgery (R0) is not possible and in patients with recurrent disease [15].

The role of imaging in malignant tumours is to stage a tumour according to the TNM classification and to assess the feasibility of surgery, which is the primary treatment of most salivary gland tumours. Imaging provides information about location (intra- or extraglandular, superficial or deep to the facial nerve), local extension and invasion, the nature of a tumour, the presence of perineural spread (PNS) and nodal and/or distant metastases, all of which affect surgical management decisions. Malignant primary salivary gland tumours are rarely multiple or bilateral. However, bilateral, multifocal involvement may occur in malignant lymphoma or metastatic disease from non-salivary tumours; recurrent disease may also present as multifocal tumour depositions. The site of origin of a salivary gland tumour determines the initial imaging technique for diagnosis. For superficial tumours within the parotid or submandibular glands, ultrasound (US) is the preferred initial imaging technique if the lesion presents as a circumscribed mass at clinical examination and is often combined with fine needle aspiration cytology (FNAC). The diagnosis is usually obtained clinically in cases of minor salivary gland tumours arising from the upper aerodigestive tract mucosa.

Magnetic Resonance Imaging (MRI) is indicated in all patients in whom a malignant tumour is suspected clinically. If the mass cannot be depicted clearly on US or if there are signs suggesting extraglandular extension, additional MRI should be obtained.

Imaging techniques

Ultrasound

Ultrasound (US) plays an important role in the initial diagnostic work up of patients presenting with a superficial preauricular or submandibular swelling. High resolution US with Doppler technique provides excellent tissue characterization, multiplanar information and vascular pattern. US is optimal to guide fine needle aspiration cytology. However, US is limited to superficial structures and accuracy depends on specialist expertise [11]. A high variability of results has been reported for US studies, with sensitivity ranging from 62% to 84%, specificity from 88% to 96%, and accuracy from 57% to 96% [16]. While superficial parotidectomy is the treatment of choice for well-defined benign and malignant parotid tumours, further diagnostic imaging and staging may be postponed in some patients until final histologic diagnosis has become available.

US offers no advantages over MRI to stage malignant primary tumours, because deep compartments cannot be depicted and retropharyngeal lymphadenopathy and perineural spread cannot be assessed. While intraoral US with high-resolution small probes is used for staging of tongue tumours, its use for staging intra-oral minor salivary gland lesions has not been reported to the knowledge of the authors.

US-guided Fine Needle Aspiration Cytology (FNAC) may provide additional information regarding the nature of a lesion offering useful information for the management of salivary gland tumours. It enables more confident preoperative patient counselling and may reduce intraoperative and/or postoperative surprises [17]. The combination of US-imaging and FNAC is debated by Bartels et al., who found comparable results for diagnosing malignant tumours by either technique alone (US alone or US-FNAC); they found no advantages in combining the two diagnostic tests, neither in terms of sensitivity, nor specificity, nor accuracy [18]; others reported a low sensitivity of US with FNAC, for distinguishing benign from malignant neoplasms and a high variability of results among different facilities, studies and countries [19]. The negative predictive value of FNAC is reported to be low (66%), thus negative results should be treated with caution [20]. In case of failure of US-guided FNAC, a reliable diagnosis of malignancy can be obtained by US-guided core-needle biopsy (CNB), which has a sensitivity of 93% and an accuracy of 98% [21]. FNAC has the lowest results in non-neoplastic disease, where CNB may be of great value [20]. In a systematic review and meta-analysis of the literature, Witt et al. found that complications are rare when using 18G core-needles: mainly subclinical haematoma formation (8 in 512 procedures), temporary facial weakness (1 in 512 procedures) [20] and fistula formation in parotitis, not in tumours [22,23]. There have been infrequent case reports of tumour seeding following both FNAC and CNB, but studies investigating tumour seeding as a function of needle diameter are lacking [20].

Thus US-FNAC has 2 main applications: first in diagnosing primary tumours and second in staging lymph node metastases.

Magnetic resonance imaging (MRI)

Traditional MRI: Basic spin-echo (SE) technique

MRI remains the preferred imaging modality for staging a malignant salivary gland tumour because of its invaluable soft tissue contrast, its multi-planar representation and optimal anatomic display. Routine high-resolution multiplanar turbo spin-echo (TSE) T1, T2 and post contrast (Gadolinium) images with fat saturation (FS) form the basis for assessment of tumour location and loco-regional tumour mapping [11,24–27] (Fig. 1). Due to the fatty changes of the parotid gland in adults, most parotid tumours can be easily depicted on non-contrast enhanced TSET1 weighted images due to their relatively low T1 signal. Normal fat has a natural high signal on TSET1 and T2 weighted sequences, and, therefore, subtle infiltration into adjacent fat planes can be observed on non-contrast enhanced SET1 weighted images. While Gadolinium shortens relaxation time, thereby increasing the signal of the enhancing tissues, fat saturation is applied after intravenous Gadolinium to amplify the contrast difference between the enhanced lesions and normal fat. High-resolution post-Gadolinium sequences with fat saturation help in depicting subtle tumour extension, but their main function is in assessing invasion of adjacent structures and demonstrating abnormal perineural enhancement along the facial and/or trigeminal nerves, indicating perineural spread (PNS) [28,11,29].

Common imaging findings of HGMSGT are ill-defined borders (Fig. 2), invasion into adjacent tissues or compartments, low T2 signal, heterogeneous enhancement, cystic changes and central necrosis [11]. Highly malignant, fast growing tumours, such as parotid duct cancer, may sometimes look like a cystic tumour, due to extensive necrosis [30]. Low-grade malignant tumours may resemble benign lesions [31,28]. Lymph node metastases are more commonly seen in HGMSGT than in low-grade tumours. The size of a malignant tumour is correlated with its high-grade or low-grade nature and with the occurrence of distant metastases [14]: tumours, that are clinically less than 4 cm having a better prognosis than tumours greater than 4 cm [1].

Selected imaging features such as cystic components or rim enhancement have been subjected to further investigation. Kato et al. [27] reported a series of 72 patients, presenting with 44 benign and 28 malignant parotid gland tumours. Cystic components were seen in 22/44 (50%) benign and 22/28 (78%) malignant
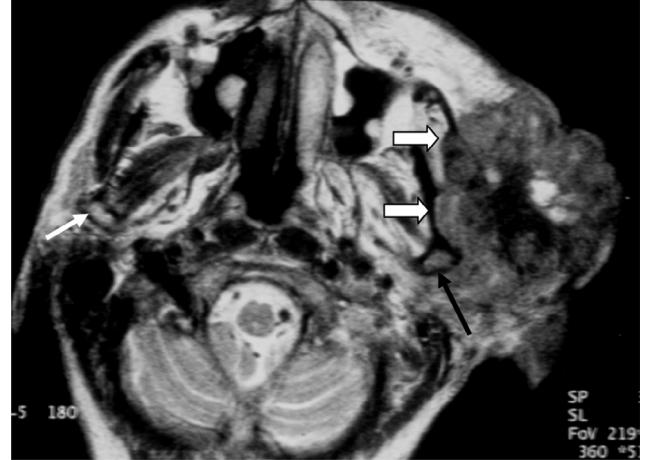
Fig. 2. Highly malignant parotid tumour on the left in 72 yrs female, who had been diagnosed with pleomorphic adenoma 18 yrs earlier but refused surgery at that time. Facial nerve palsy, pain and ulcerations. Note the heterogeneous aspect, the low T2 signal and the aggressive invasion of the masticator space (thick arrows) and alteration of normal fat signal of the bone marrow in the left mandible (black arrow; compare to normal right side: white arrow). Histology: carcinoma ex pleomorphic adenoma.
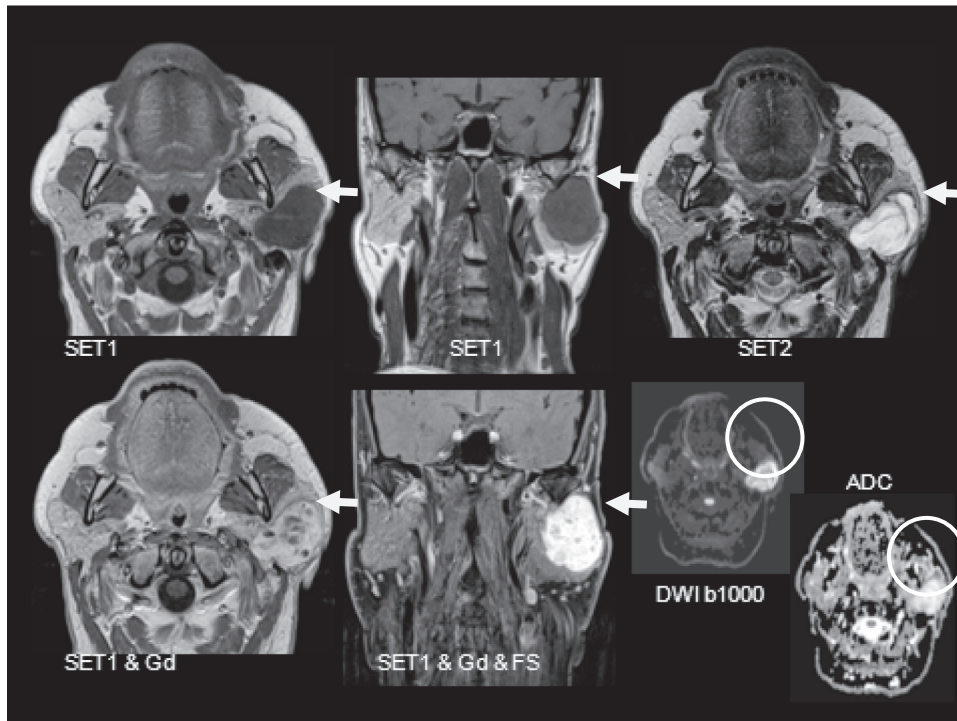
Fig. 1. M, 56 yrs, pre-auricular swelling, slowly increasing in size over months. Standard MRI protocol: SET1, TSET2, post Gadolinium without and with fat saturation, DWI (b1000) ADC. Note the well-defined, large tumour in the superficial lobe of the left parotid gland (arrows). There is no invasion of adjacent compartments. Note the lobulated aspect, high T2 signal, heterogeneous, strong enhancement after Gadolinium. High signal on b1000 in combination with high signal on ADC (white circle) suggests benign or low-grade malignant disease. Histology: benign pleomorphic adenoma.

tumours. Eccentric location of the cystic areas was noted in 20/22 benign and in 12/22 of malignant tumours, whereas central cystic areas were seen only in malignant tumours. The differences were statistically significant ($p < 0.001$). Hyperintense T1 signal also was considered a discriminative feature of benign tumours, mostly due to haemorrhagic or proteinaceous contents or many small cysts, whereas T2 signal did not differ significantly between the two groups.

Sakamoto et al. [26] analysed capsule-like rim enhancement (CLRE) on post-Gadolinium SET1 MRI of 100 patients with parotid tumours and compared this to histologic findings. CLRE was observed in 74 patients, in 51/66 (77%) benign and in 23/34 (67%) malignant tumours. They found that irregular thickening and peripheral nodules within the wall were seen more commonly in malignant tumours. The optimal cut-off value to discriminate between benign and malignant lesions was at 1.5 mm wall thickness with a sensitivity of 78%, specificity of 78% and accuracy of 78% ($p < 0.001$). Excluding Warthin tumours, 5/23 (22%) malignant lesions showed a thin rim, while a thick rim was observed in 3/51 (8%) benign lesions. Warthin tumours could not be differentiated from malignant tumours on the basis of the CLRE alone, but could be distinguished using diffusion and/or dynamic contrast-enhanced MRI techniques. The authors conclude, using a cut-off wall thickness of 1.5 mm, CLRE is a valuable measurement to further differentiate malignant from benign tumours on SET1 weighted post-Gadolinium sequences.

Perineural spread (PNS) can be observed on pre- and post-Gadolinium sequences. Imaging features of PNS include replacement of fat in neural foramina and diffuse or nodular thickening and pathologic enhancement of the named cranial nerves [32,29,11]. Both CT and MR can detect perineural spread (PNS), but MR is the modality of choice due to its superb soft tissue contrast (Fig. 3). Regarding salivary gland tumours the most commonly involved nerves in early PNS are the facial (VIIth) and trigeminal (Vth) nerves which are closest to the major salivary glands, with the auriculo-temporal nerve serving as an important connection. However, in extensive disease, other cranial nerves may become involved as well. High-resolution post-contrast fat-suppressed T1 weighted sequences are recommended [33,29]. Direct signs of nerve abnormality are detectable by this MR technique, namely the segmental nerve enhancement due to neoplastic disruption of the blood-nerve-barrier leading to increased permeability (Fig. 4). The sensitivity of MRI for PNS along cranial nerves is greater than that of CT, ranging from 70% to 95% [34,35]. Observed limitations of MRI are the false positive findings caused by changes due to inflammatory or granulomatous disease, reducing specificity to about 85%; incomplete mapping of all nerves involved – per patient – may drop the sensitivity to 20–37% [36]. Microscopic neoplastic infiltration below the resolution of MRI technique may account for some inaccuracy of PNS mapping and may explain the presence of skip lesions. MRI is the technique of choice to assess intracranial PNS spread along the Vth nerve to Meckel's cave and cavernous sinus or along the VIIth nerve to the geniculate ganglion. To assess direct intracranial extension via the skull base or direct invasion of the skull base is one of the main goals of imaging today, being of utmost importance in planning appropriate treatment. Permeative invasion into spongiotic/diploic bones (mandible, skull base) may manifest as extensive replacement of medullary fat spaces in the absence of gross cortical erosions. Such findings are more easily detected with MRI. The plain SET1 sequence is by far superior to CT [37,38].

3D post-contrast volume imaging

In recent years ultrafast 3D gradient echo sequences have been developed, providing better anatomic detail and offering multiplanar reconstructions. Different manufacturers have given this technique varying acronyms (e.g. VIBE, THRIVE, LAVA-FLEX, RADIANCE for 1.5 T and 3 T systems). Multiplanar reconstructions are obtained from a volume stack of ultra-thin (0.4–0.8 mm), isotropic, axial images instead of performing many additional series in different planes [39]. Flow-related artefacts are significantly reduced compared to spin-echo techniques [40]. However, compared to spin-echo techniques, this volumetric technique is still prone to greater patient motion and susceptibility artefacts (e.g. from dental works). Wu et al. [41] compared a more robust 3D fat-suppressed technique with standard post-contrast spin-echo T1 sequences and reported a significant improvement of tumour delineation, degree of fat suppression, mucosal enhancement and lesion edge-sharpness. This 3D fat-suppressed technique is very useful for delineating subtle tumour extension to the skull base, along cranial nerves or intracranially. These 3D sequences may also be helpful for measuring tumour volume as an expression of treatment success or failure. Kataoke et al. conclude that 3D VIBE is an acceptable alternative to post contrast spin-echo T1 weighted sequences [42].

Functional MRI techniques

Diffusion weighted imaging (DWI) provides information about the nature of a tumour, often before final histologic diagnosis has
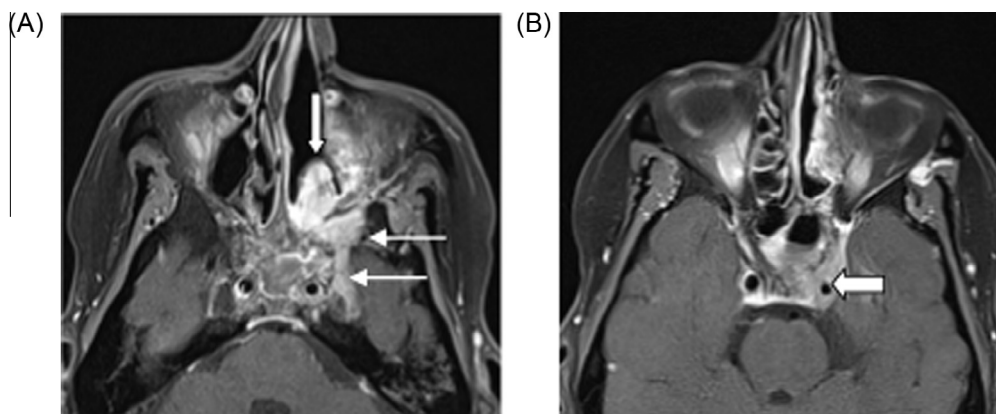
Fig. 3. (A and B) Axial SET1 post Gadolinium with fat saturation. Patient operated for adenoid cystic carcinoma of minor salivary glands in the nasal cavity. Presents with recurrent tumour. Recurrent tumour in left nasal cavity (thick arrow). Perineural tumour spread (PNS) along the branches of the left trigeminal nerve: thickening of the V-2 along its course in the pterygopalatine fossa through the round foramen into the cavernous sinus (A. small arrows). Note the compression of the internal carotid artery on the left (B. thick arrow). No clinical symptoms related to PNS.
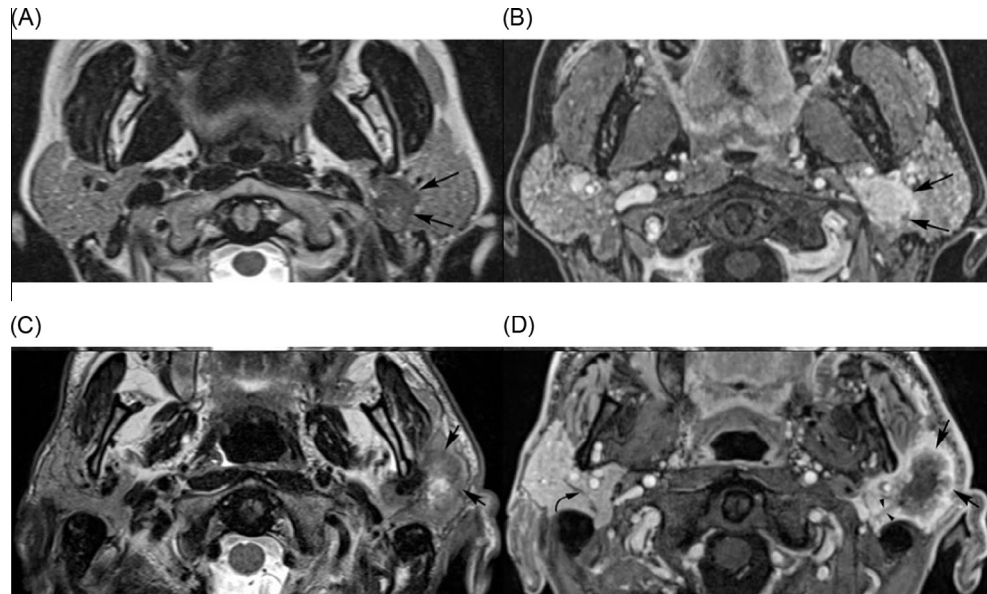
Fig. 4. (A and B) Low-grade mucoepidermoid carcinoma of left parotid gland. The tumour is located in the deep portion of the gland, shows hypointense signal on TSE T2 (A) and quite homogeneous enhancement post contrast administration on VIBE (B). Arrows on A and B point to the irregular, though well defined, outline of the tumour. (C and D) Ductal carcinoma of left parotid gland. The tumour shows heterogeneous signal with central necrosis on both TSE T2 (C) and post contrast VIBE (D). The whole gland is invaded (arrows on C and D). Arrowheads on D indicate the possible course of a thickened and fuzzy left facial nerve. Compare with the normal one in a similar position within the right gland (curved arrow on D).

been obtained. The term "molecular diffusion" refers to the random translational motion of molecules (also called Brownian motion) that results from the thermal energy carried by these molecules – a physical process that was well characterized by Einstein [43]. Free water molecules normally contribute to signal formation in MRI. Diffusion weighted imaging (DWI) is a technique that expresses freedom of motion of water molecules in intercellular spaces and relates to cellular density of tissues. Motion is reduced in highly cellular tissues and very thick fluids (abscess) but in clear fluids (cysts) no motion restriction is observed. Signal intensity is plotted against resonance time at b0 (at the start) and b1000 (at the latest) and apparent diffusion coefficient (ADC) values can be calculated [44]. Highly cellular tumours contain few free water molecules in the intercellular spaces, which results in diffusion restriction that can be seen as a high signal spot on the b1000 images and a corresponding area of low signal on the ADC map. Low-grade tumours normally show low signal on b1000 images and relatively high ADC values representing a low degree of diffusion restriction, findings that overlap with benign lesions. Most high-grade malignant tumours show a high degree of diffusion restriction, overlapping with benign tumours, where malignant lymphoma is characterized by extremely low ADC values, but in all series overlap exists between malignant and Warthin tumours, due to their high cellularity [45,8,46].

In 2009, Habermann et al. [47] reported on a larger series of 136 patients, 87 with a benign and 49 with an epithelial malignant parotid tumour. Mean ADC values for malignant tumours varied between 0.79 and $1.10 \times 10^{-3}/mm^2/s$, which was significantly lower than the ADC values of pleomorphic adenomas ($2.09 \times 10^{-3}/mm^2/s$). However, there was overlap, with Warthin tumours having a mean ADC value of $0.89 \times 10^{-3}/mm^2/s$. They concluded that due to overlapping ADC values between benign and malignant tumours and overlap within the groups, diagnosis on the basis of ADC maps alone is not possible.

In view of these data, and considering the short duration of DWI sequences, there is a strong tendency to incorporate DWI in routine MR imaging protocols and to use ADC maps as a non-invasive indicator of malignancy [46].

Dynamic Contrast-Enhanced MRI (DCE-MRI) is a technique in which the degree of tumour enhancement is plotted against time. Time-to-peak enhancement (T-peak) and a washout ratio (WR) are useful parameters to differentiate benign from malignant tumours. Yabuuchi et al. [48] reported on DCEMRI in 29 patients (33 salivary gland tumours) and proposed a classification according to 4 different time intensity curves (TIC): type A (T-peak of >120 s without WR) representing benign disease, type B (T-peak > 120 s and WR > 30%) representing Whartin's tumours, type-C (T-peak < 120 s and a WR < 30%) representing malignant and benign tumours and type-D, a flat line, representing cysts. Most malignant tumours showed a type-C curve, but a small number showed a type-B curve. When type A, B and D are considered benign and type C malignant, a high sensitivity (91%) and specificity (91%) for differentiating between benign and malignant tumours was found, but overlap existed in type-B and type C lesions, consistent with other studies [49,50]. Yabuuchi et al. [25] obtained better results combining DCEMRI with ADC maps in a series of 50 lesions (14 malignant, 36 benign) with sensitivity increasing from 71% to 86%, specificity from 86% to 97%, accuracy from 82% to 92%, PPV from 67% to 92% and NPV from 89% to 94%. Espinoza et al. [51] proposed an algorithm for MRI interpretation using diffusion and perfusion (DCEMRI). Using T1 signal and perfusion curves, they were able to single out Warthin tumours from other tumours. T2 signal, ADC maps with cut-off values <1, 1–1.3, >$1.3 \times 10^{-3}/mm^2/s$, and perfusion curves were used to separate benign from malignant tumours.

For lesions, that are suspected of being malignant, adding ADC and DCE MRI is an invaluable tool to obtain a correct diagnosis before surgery.

Intravoxel incoherent motion (IVIM) MRI

Sumi et al. [40] reported on a series of 31 epithelial salivary gland tumours, 20 benign and 11 malignant. They used an MRI technique called IVIM, in which diffusion and perfusion data are integrated [52]. They showed good results for discriminating

Warthin tumours from pleomorphic adenomas and benign from malignant tumours. They conclude that pixel-based ADC and DCE series can eliminate artefacts from heterogeneous tumours and therefore effectively discriminate benign from malignant salivary gland tumours.

Functional MRI (fMRI)

Although research has been done in applying functional MRI (fMRI) techniques (diffusion tensor fiber tractography) on the large cranial nerves (Vth, IInd), this technique has not yet become routine in daily practice [53]. As yet, fMRI has no clinical relevance for the staging of primary malignant salivary tumours.

MR-spectroscopy

A recent study suggests that MR spectroscopy may differentiate benign from malignant salivary gland tumours as well as distinguishing Warthin's tumour from pleomorphic adenoma. However, its role in routine clinical practice is not well established [54,11].

### Contrast-enhanced computer tomography (CECT)

Contrast-enhanced CT (CECT) is requested in patients in whom MRI is contra-indicated (e.g. cardiac pacemaker, claustrophobia, ferrometallic prostheses or corpora aliena) or may serve as an additional examination when MRI has questionable findings regarding bony structures of the skull base, orbit or mandible. Thin slices (0.6–1.0 mm) and multiplanar reconstructed images of the head and neck are routinely obtained using bone and soft tissue algorithms. However, soft tissue detail is inferior compared to MRI and perineural tumour extension may only be appreciated in cases of asymmetry of skull base foramina, which are caused by thickening of the nerve and erosion of the bony canal. Advantages of CECT over MRI are, that the examination is of much shorter duration, and, if necessary, the image volume can be extended to include the lungs and the abdomen. However, intravenous injection of iodinated contrast can cause allergic reactions in some patients and contrast nephropathy has also been reported after CECT in patients at risk [55,56]. Therefore patients should be screened for the risk of contrast-allergy and/or contrast-induced nephropathy by assessing renal function and related risk factors before the examination. These complications are observed in a much smaller number of patients after injection of Gadolinium for MRI examination [57].

^{18}FDG-PET CT/^{18}FDG PET-MRI

^{18}FDG PET-CT

Salivary gland tumours are an uncommon clinical indication for ^{18}FDG PET/CT and published data are still limited and mainly based on the use of ^{18}Fluorodeoxyglucose (FDG) as a metabolic imaging radiotracer. ^{18}FDG PET/CT is not useful to discriminate between benign and malignant salivary gland tumours because benign tumours, such as Warthin's tumour, may also show high glucose metabolism [58]. Distant metastases at presentation are reported in 23% of patients with a low-grade tumour compared to 36% in patients with a high-grade malignant tumour [14]. The role of ^{18}FDG PET/CT in the initial staging of salivary gland tumours is currently controversial. However, early detection of distant metastases is one of the advantages of ^{18}FDG PET/CT and recent studies have demonstrated that this imaging modality has a significant effect on the management of patients with high-grade malignant salivary gland tumours, in whom distant metastases are seen more frequently [59–63]. ^{18}FDG PET/CT is not recommended for the routine evaluation of low-grade malignant tumours, due to their low-avidity for ^{18}FDG [64]. In malignant tumours with slow development but tendency for local invasion and final poor prognosis, the use of ^{11}C-methionine PET/CT might be considered. Methionine is a neutral aminoacid that plays a key role in cancer cell metabolism, and its uptake is often enhanced, even in tumours with low glucose metabolism. A recent publication suggests that PET imaging with this radiotracer could be useful for selecting an optimally
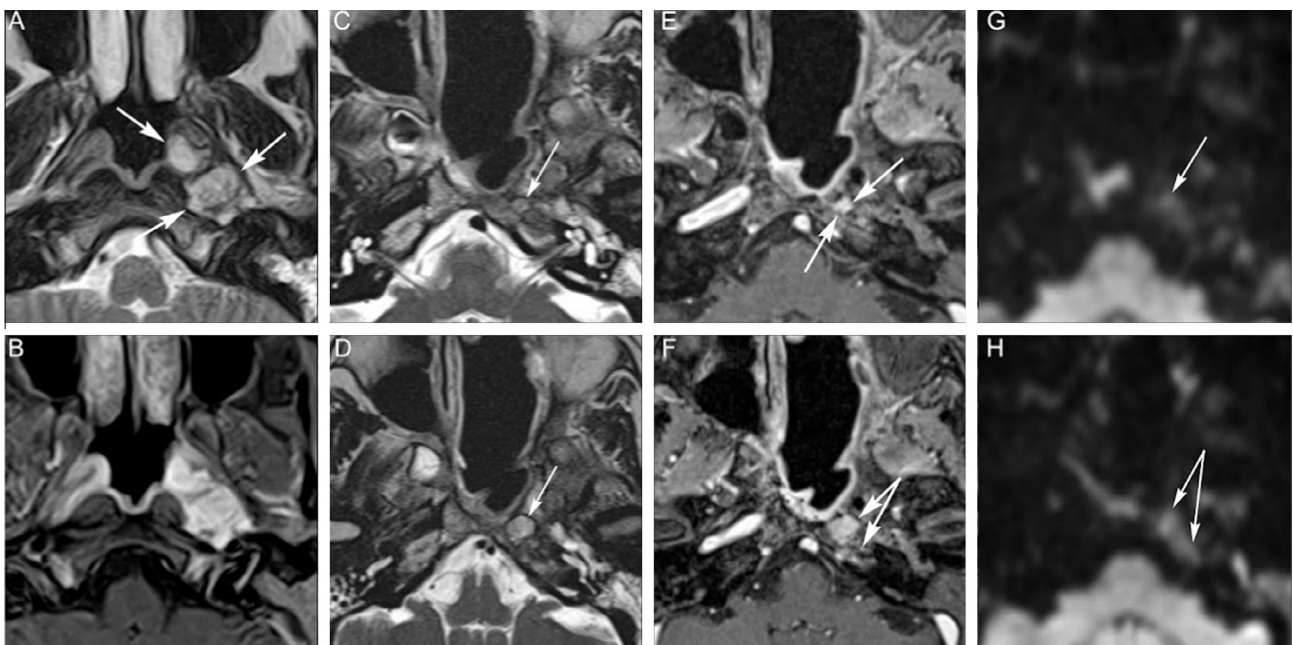
Fig. 5. (A–H). (A and B) Recurrent adenoid cystic carcinoma of minor salivary gland after chemo-radiation therapy. The tumour arises from the left wall of the nasopharynx and grows sub-mucosally (arrows in A). The signal is moderately hyperintense on TSE T2 (A) and shows homogeneous enhancement after contrast agent administration (B). C: on follow-up MR, 7 months after salvage naso-endoscopic resection, a very small nodule (arrow) is detected at the left foramen lacerum (the left internal carotid artery was occluded via endovascular embolization). D: further growth of recurrent tumour is observed at the second follow-up, 10 months after salvage surgery (arrow). The recurrence shows greater enhancement (arrows on E and F) and abnormal signal on b1000 (arrows on G and H) than surrounding tissues both at 7 and 10 months.

individualized treatment strategy in patients affected by primary adenoid cystic carcinomas of the head and neck. The authors demonstrated that high residual post-radiotherapy tumour uptake was a significant factor for predicting cancer recurrence, and they speculated that this information might be used to select those patients deserving a strict short-term follow-up and/or active combination of other treatments [65]. The major limitation of these tracers is that, unfortunately, their use is restricted to PET centers with in-house cyclotron and radiochemistry laboratories because of the short half-life of [11]C.

[18]FDG PET-MRI is a new imaging technique combining functional imaging with anatomic information. This is a highly sophisticated and complex technique [66,67]. As of now no clinically applicable results use have been published for patients with salivary gland tumours.

Follow-UP – introduction

After curative treatment for high-grade malignant salivary gland tumours (HGMSGT) clinical examination is impeded by altered anatomy and fibrosis. Recurrences, especially within the deep compartments of the face, and perineural spread may go unnoticed clinically at its earliest stage (Fig. 5). Seventy percent of recurrences of HGMSGT are seen within 3 years of treatment [3,4]. In a large study of 565 patients with salivary gland cancer Terhaard reported 13% local recurrences (Fig. 6), 22% regional recurrences and 33% distant metastases during a follow-up period of 10 years [13]. Distant metastases are reported in >50% by others in smaller series [68,60] and are most commonly seen in high grade ACC, adenocarcinoma NOS and carcinoma ex pleomorphic adenoma [3]. Up to 90% of distant metastases are located within the lungs (Fig. 7), 15% in the bones and 5% in liver, brain or other sites (skin). Follow-up periods are reported from 3 to 10 years or lifelong [3,4,69]. Prognosis for any treated patient with progressing or relapsing disease is poor, regardless of cell type or stage [6]. The efforts in surveillance should focus in particular on recurrences whose detection may have clinical consequences, i.e. that are still treatable with a curative intention [3,4,69].

Imaging during follow-up

Ultrasound

Ultrasound (US) is a quick means to differentiate solid from cystic lesions in the superficial areas of the head and neck. US guided FNAC may help establishing the diagnosis of recurrent disease or non-malignant complications. However, US has a limited contribution because deep compartments cannot be addressed.
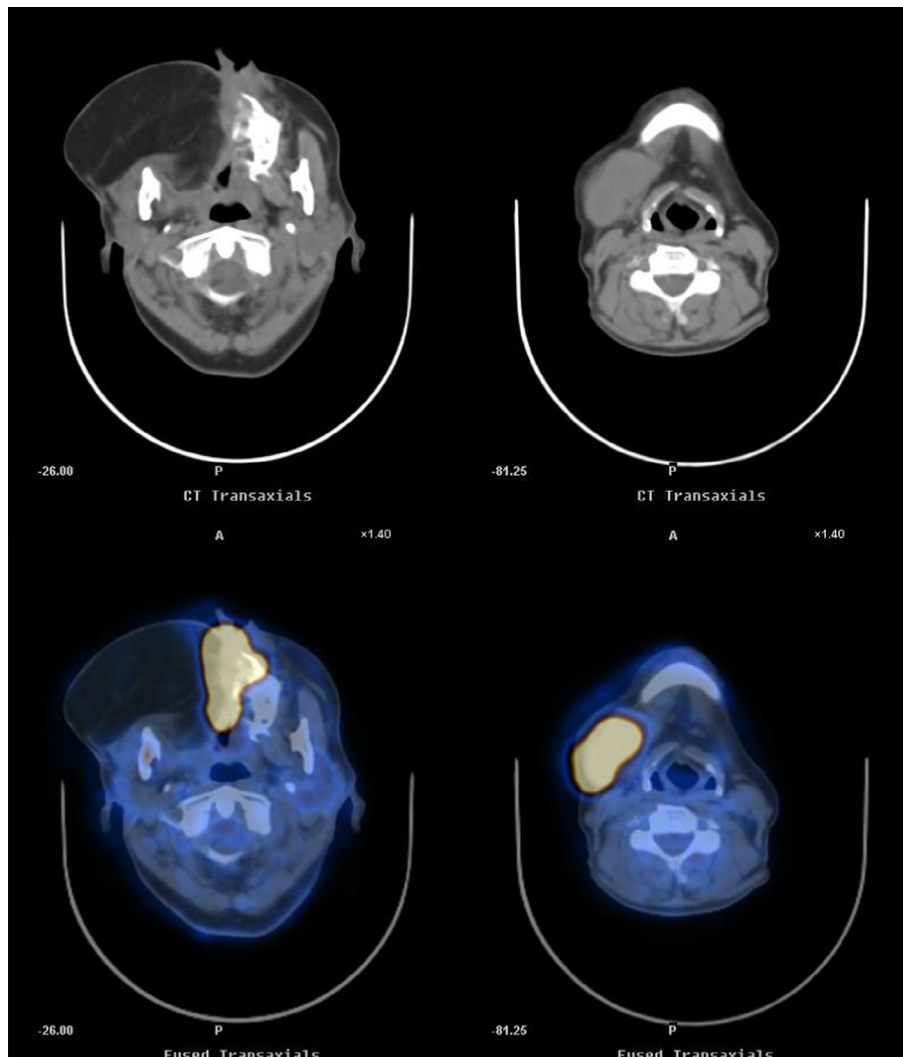
Fig. 6. (A–D) [18]FDG-PET CT in recurrent adenoid cystic carcinoma. Postoperative changes with fat flap on the right (arrow). Non-enhanced CT images (A and B) and FDG-PET (C and D). Large FDG-avid recurrent tumour at the medial border of the resection area (arrows). Large submandibular metastatic lymph node on the right (arrow).
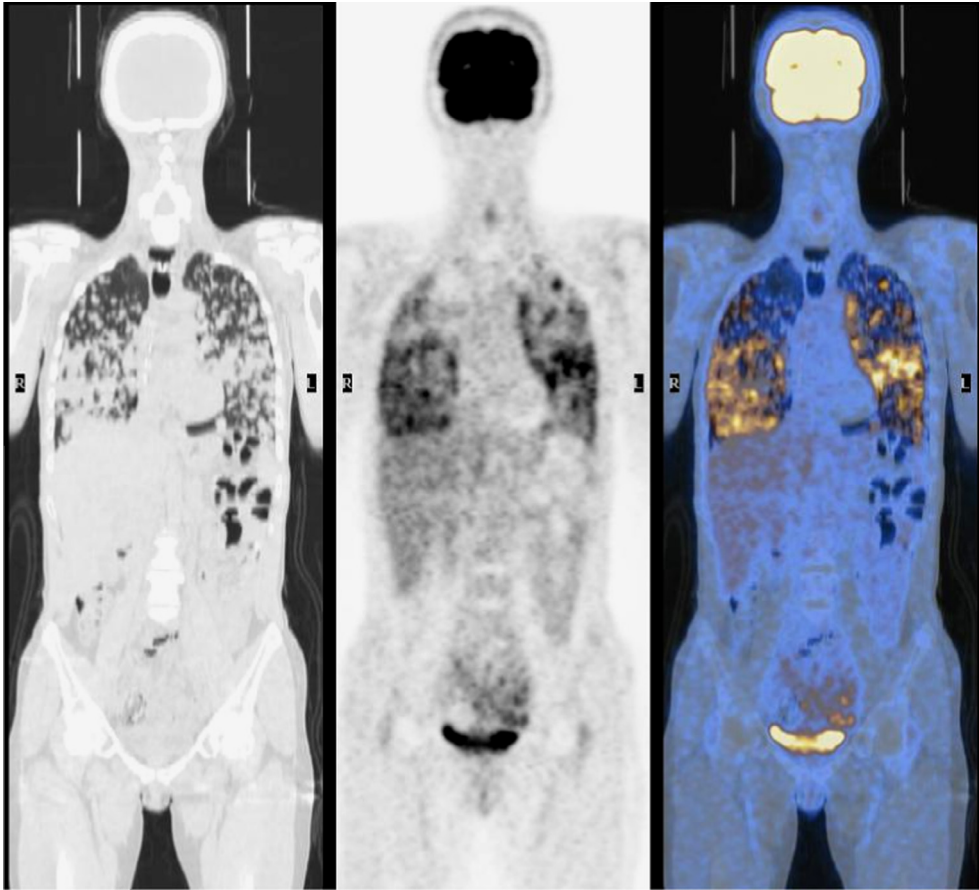
Fig. 7. (FC) [18]FDG-PET CT: multiple, FDG-avid lungmetastases at presentation in a patient with adenoid cystic carcinoma.

MRI

With the rapid development of cross sectional imaging techniques (DWI-ADC, DCE-MRI) and the increasing availability of MRI and [18]FDG PET/CT, a baseline imaging study (MRI or CECT) is recommended by some authors [3] to facilitate early recognition of recurrent disease during follow-up, but there are no evidence-based studies to support this strategy. Extensive anatomic changes are commonly observed after surgery and/or radiation therapy. A baseline study at 3 months after completion of therapy can serve as an invaluable road map for early detection of recurrent tumour; the level of confidence to demonstrate or exclude recurrent disease is higher than without a comparable baseline examination. Although different authors have demonstrated the value of post-treatment baseline studies for squamous head and neck cancer [70], to the knowledge of the authors no such study for HGMSGT is available as yet. MRI, with intravenous Gadolinium, is advised for loco-regional assessment due to its excellent depiction of the soft tissues. Diffusion weighted imaging may be helpful in monitoring treatment [71,46] and in identifying recurrent disease, as has been reported for squamous cell cancers of the head and neck. MRI with intravenous contrast is the only way to demonstrate perineural spread along named cranial nerves, which is more often seen in recurrences of high-grade malignant salivary tumours.

[18]FDG-PET/CT

Although [18]FDG-PET/CT is reported as having a high diagnostic contribution at initial staging with a change of treatment planning in up to 15–25% of patients [58,3] recent papers do not demonstrate a significant contribution during surveillance, due to false negative and false positive results [62,63,72,58]. However, [18]FDG PET/CT is superior to other cross-sectional imaging techniques to demonstrate (occult) distant metastases and/or second primary tumours [3]. Espinoza et al. [51] suggest that the best technique for detecting recurrences appears to be [18]FDG-PETCT combined with DCE-MRI, and that a new rise in tissue blood flow (TBF) after radiochemotherapy could differentiate between recurrent disease and non-specific post-treatment changes. But their preliminary results should be confirmed by larger studies. There is no consensus on the necessity or the frequency of routine imaging during follow-up (chest X-ray, chest CT, MRI, DWI-MRI, [18]FDG PET/CT) and the costs are considered high [69,73,74]. There is no evidence-based study that favours routine – yearly – long-term imaging follow-up in patients with HGMSGT. Although only palliative treatment can be offered in patients with a large tumour load, metastasectomy in oligometastatic disease, e.g. solitary lung metastasis in ACC, can improve survival in some selected patients, but due to the small numbers studied, the results of this strategy remain difficult to assess statistically. However, during the last Consensus Meeting on HGMSGT in Brescia, October 2014, it was suggested that follow-up CT of the chest is preferred to chest X-ray in patients who may benefit from chemotherapy, so as to better stage the lung nodules and follow progression or regression of disease during and after experimental medical treatment. While most recurrences of HGMSGT are seen within 2 years from primary diagnosis, this seems a reasonable and not excessively costly strategy. When loco-regional recurrence and/or distant metastases are clinically suspected, a wide spectrum of imaging techniques is used by different authors: ultrasound with FNAC is recommended by Digonnet et al. [3]. But Gillespie et al. [4] advocate MRI with Gadolinium or contrast-enhanced CT, or [18]FDG PET/CT in patients

who have a biopsy-proved recurrence. No evidence-based results are available regarding the usefulness of these different strategies, which are mainly inspired by local routine, availability and experience.

Conclusions

MRI is the most appropriate imaging technique for precise local mapping of primary malignant salivary tumours. Although new developments such as diffusion (DWI/ADC) and perfusion (DCE-MRI/IVIM) MRI suggest better differentiation among tumour types, the reported numbers are too low to draw firm conclusions. Additional US with FNAC is recommended for assessing the nature of a primary salivary gland tumour and N-staging the neck in all patients.

For the assessment of distant metastases at initial presentation [18]FDG PET/CT seems to be the most sensitive imaging technique. However, because most distant metastases do occur in the lungs, chest-CT may be considered. After completion of treatment, a base-line MRI of the head and neck is recommended in patients with high-grade malignant tumours in whom local recurrence rates are high. In patients with loco-regional recurrent disease, MRI, if possible combined with US-guided FNAC, is the preferred imaging technique to direct treatment strategies. In case of distant metastases during follow-up, chest-CT or symptom-related imaging is recommended. MRI of the head and neck in combination with CECT of the chest and abdomen plays an important role for evaluation of experimental chemotherapy in patients with advanced primary salivary gland tumours or recurrent disease.

Conflict of interest statement

The authors declare that there are no conflict of interest.

Acknowledgments

References

[1] Speight PM, Barrett AW. Salivary gland tumours. Oral Dis 2002;8(5):229–40.
[2] Wenig BM. Neoplasms of the salivary glands. In: Atlas of head and neck pathology. Saunders/Elseviers; 2008 [chapter 18:582].
[3] Digonnet A, Hamoir M, Andry G, et al. Follow-up strategies in head and neck cancer other than upper aerodigestive tract squamous cell carcinoma. Eur Arch Otorhinolaryngol 2013;270:1981–9.
[4] Gillespie MB, Albergotti WG, Eisele DW. Recurrent salivary gland cancer. Curr Treat Options Oncol 2012;13:58–70.
[5] Gnepp D. Malignant mixed tumour. In: Diagnostic surgical pathology of the head and neck. Saunders; 2009. p. 444.
[6] National Cancer Institute (NCI): PDQ (registered) Salivary gland cancer treatment. Bethesda, MD. Health professional version dd 12 March; 2014.
[7] Ellis GL, Auclair PL. Tumours of the salivary glands. In: Atlas of tumour pathology. Washington DC: Armed Forces Institute of Pathology; 1996. p. 3.
[8] Kato H, Kanematsu M, Goto H, et al. Mucosa-associated lymphoid tissue lymphoma of the salivary glands: MR imaging findings including diffusion-weighted imaging. Eur J Radiol 2012;81:e612–7.
[9] Dispenza F, Cicero G, Mortellaro G, et al. Primary non-hodgkins lymphoma of the parotid gland. Braz J Otorhinolaryngol 2011;77(5):639–44.
[10] Ekstrom-Smedby K. Epidemiology and etiology of non-Hodgkin lymphoma – a review. Acta Oncol 2006;45:258–71.
[11] Lee YY, Wong KT, King AD, Ahuja AT. Imaging of salivary gland tumours. Eur J Radiol 2008;66:419–36.
[12] Nuyens M, Schüpbach J, Stauffer E, Zbären P. Metastatic disease to the parotid gland. Otolaryngol Head Neck Surg 2006;135:844–8.
[13] Terhaard CH, Lubsen H, Van der Tweel I, et al. Salivary gland carcinoma: independent prognostic factors for locoregional control, distant metastases and overall survival: results of the Dutch Head and Neck Oncology Cooperative Group. Head Neck 2004:681–93.
[14] Gao M, Hao Y, Huang MX, et al. Clinicopathological study of distant metastases of salivary adenoid cystic carcinoma. Int J Oral Maxillofac Surg 2013;42:923–8.
[15] Cerda Th, Sun Xu Shan, Vignot S, et al. A rationale for chemoradiation vs radiotherapy in salivary gland cancers? Crit Rev Oncol/Hematol 2014;91:142–58.
[16] Bozzato A, Zenk J, Greess H, et al. Potential of ultrasound diagnosis for parotid tumors: analysis of qualitative and quantitative parameters. Otolaryngol Head Neck Surg 2007;137:642–6.
[17] Wong DY, Li GKH. The role of fine needle aspiration cytology in the management of parotid tumours: a critical clinical appraisal. Head Neck 2000:469–72.
[18] Bartels S, Talbot JM, DiTomasso J, et al. The relative value of fine-needle aspiration and imaging in the preoperative evaluation of parotid masses. Head Neck 2000:781–6.
[19] Schmidt RL, Hall BJ, Layfield LJ. A systematic review and meta-analysis of the diagnostic accuracy of ultrasound-guided core needle biopsy for salivary gland lesions. Am J Clin Pathol 2011;136(4):516–26.
[20] Witt BL, Schmidt RL. Ultrasound-guided core needle biopsy of salivary gland lesions: a systematic review and meta-analysis. Laryngoscope 2013;124(3):695–700.
[21] Novoa E, Gurtler N, Arnoux A, et al. Role of ultrasound-guided core-needle biopsy in the assessment of head and neck lesions: a meta-analysis and systematic review of the literature. Head Neck 2012;34(10):1497–503.
[22] Wan Y-L, Chan S-C, Cheung Y-C, et al. Ultrasonography-guided core needle biopsy of parotid gland masses. AM J Neuroradiol 2004;25:1608–12.
[23] Song IH, Song JS, Sung CO, et al. Accuracy of core needle biopsy versus fine needle aspiration cytology for diagnosing salivary gland tumours. J Pathol Transl Med 2015;49:136–43.
[24] Christe A, Waldherr C, Hallett R, et al. MR imaging of parotid tumours: typical lesion characteristics in MR Imaging improve discrimination between benign and malignant disease. AJNR 2011;32:1202–7.
[25] Yabuuchi H, Matsuo Y, Kamitani T, et al. Parotid gland tumours: can addition of diffusion weighted MRI to dynamic contrast-enhanced MRI improve diagnostic accuracy in characterization? Radiology 2008;249(3):909–16.
[26] Sakamoto M, Likubol M, Sasano T, et al. Diagnostic value of capsule-like rim enhancement on magnetic resonance imaging for distinguishing malignant from benign parotid tumors. Int J Oral Maxillofacial Surg 2014;43:1035–41.
[27] Kato H, Kanematsu M, Watanabe H, et al. Salivary gland tumors of the parotid gland: CT and MRI imaging findings with emphasis on intratumoral cystic components. Neuroradiology 2014;56:789–95.
[28] Thoeny H. Imaging of salivary gland tumours. Cancer Imag 2007;7:52–62.
[29] Maroldi R, Farina D, Borghesi A, et al. Perineural tumor spread. Neuroimag Clin N Am 2008;18:413–29. xi.
[30] Weon YC, Park SW, Kim HJ, et al. Salivary duct carcinomas: clinical and CT and MR imaging features in 20 patients. Neuroradiology 2012;54:631–40.
[31] Freling NJ, Molenaar WM, Vermey A, et al. Malignant parotid tumors: clinical use of MR imaging and histologic correlation. Radiology 1992;185(3):691–6.
[32] Sigal R, Monnet O, de Baere T, et al. Adenoid cystic carcinoma of the head and neck: evaluation with MR imaging and clinical-pathologic correlation in 27 patients. Radiology 1992;184:95–101.
[33] Hanna E, Vural E, Prokopakis E, et al. The sensitivity and specificity of high-resolution imaging in evaluating perineural spread of adenoid cystic carcinoma to the skull base. Arch Otolaryngol Head Neck Surg 2007;133:541–5.
[34] Nemzek WR, Hecht S, Gandour-Edwards R, et al. Perineural spread of head and neck tumors: how accurate is MR Imaging? AJNR Am J Neuroradiol 1998;19:701–6.
[35] Shimamoto H, Chindasombatjaroen J, Kakimoto N, et al. Perineural spread of adenoid cystic carcinoma in the oral and maxillofacial regions: evaluation with contrast-enhanced CT and MRI. Dentomaxillofac Radiol 2012;41(2):143–51. http://dx.doi.org/10.1259/dmfr/21825064 PMCID: PMC3520370.
[36] Farina D, Maroldi R. Neoplasms of the sinonasal cavities. In: Hermans R, editor. Head and neck cancer imaging. Berlin; New York: Springer; 2006. p. 207–35.
[37] Suei Y, Tanimoto K, Taguchi A, et al. Primary intraosseous carcinoma: review of the literature and diagnostic criteria. J Oral Maxillofac Surg 1994;52:580–3.
[38] Tomura N, Hirano H, Sashi R, et al. Comparison of MR imaging and CT in discriminating tumor infiltration of bone and bone marrow in the skull base. Comput Med Imag Graph 1998;22:41–51.
[39] Ahn SS, Kim J, An C, et al. Preoperative imaging evaluation of head and neck cancer: comparison of 2D spin-echo and 3D THRIVE MRI techniques with resected tumors. Clin Radiol 2012;67:e98–e104.
[40] Sumi M, Van Cauteren M, Sumi T, et al. Salivary gland tumours: use of intravoxel incoherent motion MR imaging for assessment of diffusion and perfusion for the differentiation of benign from malignant tumours. Radiology 2012;263(3):770–7.
[41] Wu X, Raz E, Block TK, et al. Contrast-enhanced radial 3D fat-suppressed T1 weighted gradient-recalled echo sequence versus conventional fat-suppressed contrast-enhanced T1-weighted studies of the head and neck. Am J Radiol (AJR) 2014;203(Oct):883–9.
[42] Kataoka M, Ueda H, Koyama T, et al. Contrast-enhanced volumetric interpolated breath-hold examination compared with spin-echo T1-weighted imaging of head and neck tumours. Am J Radiol (AJR) 2005;184(Jan):313–9.
[43] Le Bihan D, Poupon C, Amadon A, et al. Artifacts and pitfalls in diffusion MRI. J Mag Resonance Imag 2006;24:478–88.

[44] Thoeny HC, De Keyzer F, Boesch C, et al. Diffusion-weighted imaging of the parotid gland: influence of the choice of b-values on the apparent diffusion coefficient value. J Magn Reson Imag 2004;20:786–9.

[45] Eida S, Sumi M, Sakihama N, et al. Apparent diffusion coefficient mapping of salivary gland tumours: prediction of benignancy or malignancy. Am J Neuroradiol 2007;28:116–21.

[46] Thoeny HC, DeKeyzer F, King A. Diffusion weighted imaging in the head and neck. Radiology 2012;263(1):19–32.

[47] Habermann CR, Arndt C, Graessner J, et al. Diffusion-weighted echo-planar imaging of primary parotid gland tumours: is a prediction of different histologic subtypes possible? Am J Neuro Radiol (AJNR) 2009;30 (March):591–6.

[48] Yabuuchi H, Fukuya T, Tajima T, et al. Salivary gland tumours: diagnostic value of Gadolinium-enhanced dynamic MR Imaging with histopathologic correlation. Radiology 2003;226:345–54.

[49] Hisatomi M, Asaumi J-I, Yanagi Y, et al. Diagnostic value of dynamic contrast-enhanced MRI of salivary gland tumours. Oral Oncol 2007;43:940–7.

[50] Aghaghazvini L, Salahshour F, Yazdani N, et al. Dynamic contrast-enhanced MRI for differentiation of major salivary gland neoplasms, a 3T MRI study. Dentomaxillofac Radiol 2014:20140166.

[51] Espinoza S, Malinvaud D, Siauve N, Halimi P. Perfusion in ENT imaging. Diagnostic Interventional Imag 2013;94:1225–40.

[52] Le Bihan D, Breton E, Lallemand D, et al. Intravoxel incoherent motion perfusion MRI: a wake-up call. Radiology 2008;249(3):748–52.

[53] Kabasawa H, Masutani Y, Aoki S, et al. 3T PROPELLER diffusion tensor fiber tractography: a feasibility study for cranial nerve fiber tracking. Radiat Med 2007;25(9):462–6.

[54] King AD, Yeung DK, Ahuja AT, et al. Salivary gland tumours at in vivo proton MR spectroscopy. Radiology 2005;237:563–9.

[55] Seok-In Hong, Shin Ahn, Yoon-Seon Lee, et al. Contrast-induced nephropathy in patients with active cancer undergoing contrast-enhanced computed tomography. Support Care Cancer http://dx.doi.org/10.1007/s00520-015-2875-6.

[56] Azzalini L, Spagnoli V, Ly HQ. Contrast-induced nephropathy: from pathophysiology to preventive strategies. A review. Can J Cardiol 2015. http://dx.doi.org/10.1016/j.cjca.2015.05.013. pii: S0828-282X(15)00395-5 May 23. [Epub ahead of print].

[57] Silver SA, Shah PM, Chertow GM, et al. Risk prediction models for contrast-induced nephropathy: systematic review. BMJ 2015;27(351):h4395. http://dx.doi.org/10.1136/bmj.h4395.

[58] Park HL, Yoo IR, Lee N, et al. The value of [18]FDG PET for planning treatment and detecting recurrence in malignant salivary gland tumors: comparison with conventional imaging studies. Nucl Med Mol Imag 2013;47:242–8.

[59] Otsuka H, Graham M, Kogame M, et al. The impact of FDG-PET in the management of patients with salivary gland malignancy. Ann Nucl Med 2005;19(8):691–4.

[60] Jeong HS, Chung MK, Son YI, et al. Role of FDG-PET/CT in management of high grade salivary gland malignancies. J Nucl Med 2007;48:1237–44.

[61] Cermik TF, Mavi A, Acikgoz G, et al. FDG PET in detecting primary and recurrent malignant salivary gland tumors. Clin Nucl Med 2007;32(4):286–91. http://dx.doi.org/10.1097/01.rlu.0000257336.69537.cb.

[62] Razfar A, Heron DE, Branstetter IV BF, et al. Positron emission tomography-computed tomography adds to the management of salivary gland malignancies. Laryngoscope 2010;120(4):734–8.

[63] Kim JY, Lee SW, Kim JS, Kim SY, et al. Diagnostic value of neck node status using ^{18}F-FDG PET for salivary duct carcinoma of the major salivary glands. J Nucl Med 2012;53(6):881–6.

[64] Bui CD, Ching ACS, Carlos RC, et al. Diagnostic accuracy of 2-[Fluorine-18] Fluoro-2-Deoxy-D-glucose positron emission tomography imaging in non-squamous tumors of the head and neck. Invest Radiol 2003;38(9):593–601.

[65] Toubaru S, Yoshikawa K, Ohashi S, et al. Accuracy of methionine-PET in predicting the efficacy of heavy-particle therapy on primary adenoid cystic carcinomas of the head and neck. Radiat Oncol 2013;8:143.

[66] Schouten CS, de Graaf P, Alberts FM, et al. Response evaluation after chemoradiotherapy for advanced nodal disease in head and neck cancer using diffusion-weighted MRI and ^{18}F-FDG-PET-CT. Oral Oncol 2015;51 (5):541–7. http://dx.doi.org/10.1016/j.oraloncology.2015.01.017. Epub 2015 Feb 26.

[67] Varoquaux A, Rager O, Dulguerov P, et al. Diffusion-weighted and PET/MR imaging after radiation therapy for malignant head and neck tumors. Radiographics 2015;35(5):1502–27. http://dx.doi.org/10.1148/rg.2015140029. Sep–Oct. Epub 2015 Aug 7.

[68] Zhao J, Wang J, Yu C, et al. Prognostic factors affecting the clinical outcome of carcinoma ex pleomorphic adenoma in the major salivary glands. World J Surg Oncol 2013;11:180–7.

[69] Manikantan K, Khode S, Dwivedi RC, et al. Making sense of posttreatment surveillance in head and neck cancer: when and what of follow-up. Cancer Treat Rev 2009;35:744–53.

[70] Hermans R. Posttreatment imaging in head and neck cancer. Eur J Radiol 2008;66:501–11.

[71] Lambrecht, Van Herck, De Keyzer, et al. Redefining the target early during treatment. Can we visualize regional differences within the target volume using sequential diffusion weighted MRI? Radiother Oncol 2014;110 (2):329–34.

[72] Sharma P, Jain TK, Singh H, et al. Utility of ^{18}F-FDG PET-CT in staging and restaging of patients with malignant salivary gland tumours: a single-institutional experience. Nucl Med Commun 2013;34(3):211–9.

[73] Joshi A, Calman F, OÇonnell M, et al. Current trends in follow-up head and neck cancer patients in the UK. Clin Oncol 2010;22:114–8.

[74] O'Meara WP, Thiringer JK, Johnstone PA. Follow-up of head and neck cancer patients post radiotherapy. Radiother Oncol 2003;66:323–6.